VIBRATION BEHAVIOR OF
HEBER HYDROCARBON BOOSTER PUMPS

Donald W. McLaughlin

Design Consultant

John F. Nagy

Analytical Engineer

Mechanical Technology, Incorporated

Latham, New York

and

Jonne L. Berning

Project Manager

Electric Power Research Institute

Palo Alto, California

Donald W. McLaughlin received a B.S. in Mechanical Engineering from Michigan State University and an M.S. in Applied Mechanics from Rensselaer Polytechnic Institute. He has also taken additional courses in statistics, reliability, and probabilistic methods in structural design. His career has been primarily in engineering analysis as a Stress Analyst, Failure Analyst, Manager, and presently as a Design Consultant in the Research and Development Division of Mechanical Technology, Incorporated.

The results of Mr. McLaughlin's work have been published in six technical papers and articles and over fifty internal technical reports. He also is a regular lecturer at MTI technical seminars on rotating machinery dynamics and investigation of machinery failure.

John F. Nagy received a B.S. in Mechanical Engineering and an M.S. in Mechanical Engineering from Rensselaer Polytechnic Institute. He has also taken courses in Business Administration. He works as an Analytical Engineer for the Research and Development Division of Mechanical Technology, Incorporated. His specialties include rotordynamics, stress analysis, lubrication and vibration. He has authored or co-authored over thirty MTI Technical Reports and is director of MTI's Rotating Machinery Dynamics Seminar.

Jonne L. Berning received his B.S. in Ocean Engineering in 1978 from Florida Institute of Technology. After graduation he spent six years working for several companies in the field of oil well completion and reservoir engineering. In 1980, Mr. Berning began working for W. K. Technology, as their Operations and Testing Manager for two Department of Energy geopressure production facilities. The primary goal of these geopressure facilities was methane gas recovery and reservoir definition to define the size and quality of this energy resource.

In 1985, Mr. Berning began working for the Electric Power Research Institute (EPRI) in California, as a Project Manager in the Geothermal program. At EPRI, Mr. Berning worked on Binary-Cycle power plants, Scale Control in geothermal brines and computer simulation of Geothermal power plants. Currently, EPRI has created a new division where Mr. Berning is a Project Manager for Biomass and Geothermal projects.

ABSTRACT

The Heber Project is a demonstration power plant which operates on a binary cycle using a geothermal heat source. It has four booster pumps in the hydrocarbon working fluid circuit. These pumps have had a long history of high vibration leading to a number of outages from seal and bearing failures. A particularly baffling problem was a sharp increase in vibration whenever pump load was rapidly increased.

In an effort to understand the cause of the vibration, a rotordynamic analysis of the pump was carried out. Particular attention was given to the fluid film stiffness and damping of the wear ring seals. The results of the study showed the cause of the vibration sensitivity was a first critical frequency very close to running speed. It was also shown that an unusual coupling existed between pump load and the seal stiffness and damping available to support the rotor and control its motions. A redesigned thrust balancing device was shown to provide a solution to both vibration problems.

INTRODUCTION

The Heber Geothermal Binary Demonstration Project is a 45-Mwe (net) binary-cycle demonstration power plant, located in the Imperial Valley in Southern California. The plant converts geothermal energy from a moderate-temperature, underground brine reservoir to electrical energy. Heat from the brine is transferred to a hydrocarbon working fluid, a mixture of 90 percent (mole) Isopentane and 10 percent (mole) Isopropane. The hydrocarbon vapor is expanded through a turbine which drives a generator to produce electricity.

The hydrocarbon system consists of four condensate pumps and four booster pumps. Each of the four pump sets is designed to carry 25 percent of the total capacity. The booster pumps are two stage, horizontal, 8730 gpm units. There have only been eight pumps of this design built to date. Four of these pumps are in water service as boiler feed pumps and the remaining four are in service at the Heber Binary Plant, pumping hydrocarbon.

From startup in May 1985, to the scheduled plant outage in June 1987, the four booster pumps experienced 32 failures, collectively. Mean time between failures (MTBF) was 485 hours. Failures were of the following types: increased leakage from cartridge seals, wiped journal and thrust bearings, excessive wear in wear ring seals and high vibration (2.5 to 4.0 mils peak-to-peak) during startup and during rapid load increases. The units were taken out of service to prevent serious damage whenever vibration levels reached 4.1 mils.

Despite several modifications to the pumps by the manufacturer, vibration sensitivity continued to be a problem. An extensive vibration survey in the field failed to disclose the reason for the sensitivity of the pumps and their proximity to failure.

Finally, in the Fall of 1987, a thorough lateral rotordynamic analysis of the booster pumps was undertaken in order to determine the cause of the vibration and failures. The results of that analysis are presented herein.

BACKGROUND

The pump configuration is shown in cross-section in Figure 1. The pumps exhibited two frequencies of vibration, $1\times$ running speed and $7\times$ running speed. The $7\times$ frequency was primarily a casing vibration. It was apparently due to hydraulic interaction b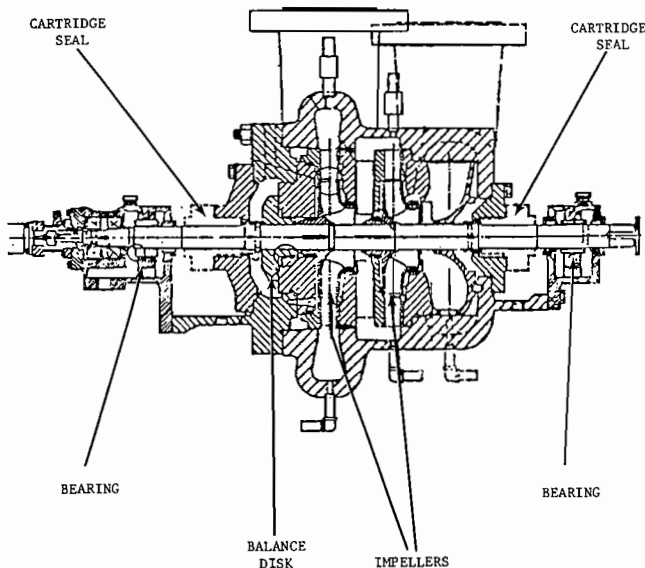etween the seven vanes on each impeller and eight diffuser vanes. Modifications to the impeller tips and clearances reduced the $7\times$ to an acceptable level. The $1\times$ vibration continued to be a problem. Rapid load increases in particular caused a sharp increase in vibration. Cartridge seal failures occurred most often on the outboard end of the pump. After some initial seal problems were solved, later seal failures were regarded as a result of high shaft vibration, not a cause of it.

Five basic modifications were made to the pumps during their operating history in an effort to reduce the $1\times$ vibration. They included changes in shaft material from steel to bronze and back to steel, and changes in labyrinth seal configurations. None of these had any appreciable affect on the shaft vibration. The final modification replaced the original balance disk with a balance piston. One pump was run for about one hour with the new configuration. Results were good. Vibration was low and no increase was seen during an inadvertent abrupt load increase.

ROTORDYNAMIC ANALYSIS

Rotor Models

Four different variations of the booster pump rotor-bearing assembly were analyzed. They had the following features:

MOD 1—Steel shaft with original balance disk (Figure 2) and five active wear-ring seals. This model represented the pump rotor-bearing-seal assembly in its original design state. All the wear-ring seals were assumed to be active, that is, they all had an axial pressure drop across them and consequently generated radial stiffness and damping.

MOD 2—Steel shaft with original balance disk and three active seals. This was similar to MOD 1, except that the balance disk was assumed to have significantly reduced clearance across its sealing surface, a condition which would result from a rapid
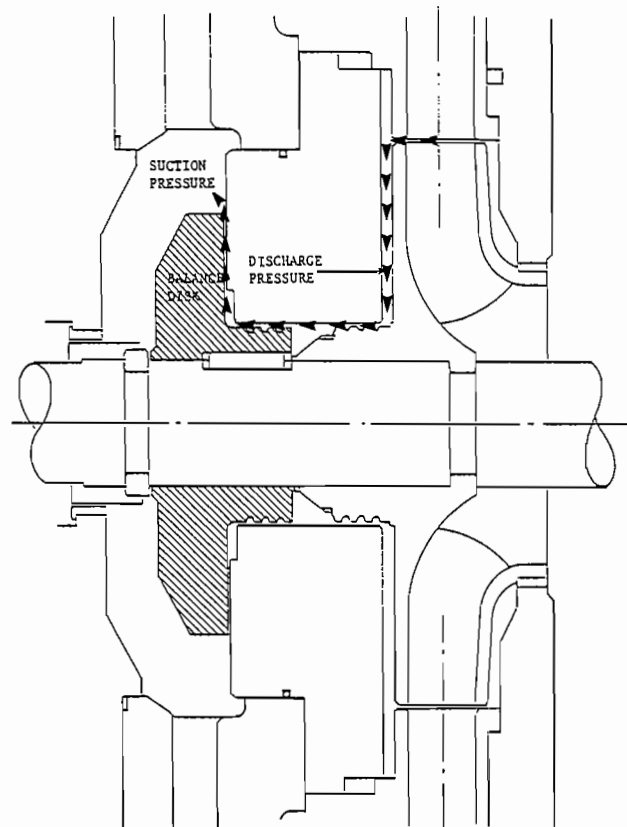

Figure 1. Pump Cross-Section.

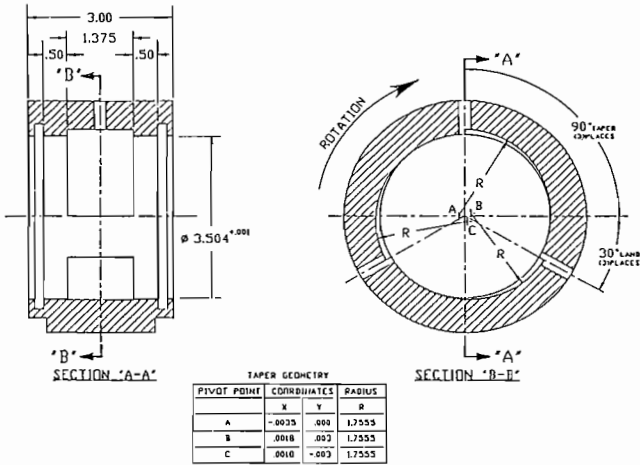Figure 2. Original Design—Balance Disk.

Figure 4. Hybrid Journal Bearing.

Steady-state and dynamic bearing data at 3600 rpm are presented in Table 2 and Table 3, respectively, for bearing number 1 which carries a load of 320 lb and bearing number two which

Table 2. Bearing 1 Steady—State and Dynamic Data

Rotor Speed = 3600.00 rpm
Bearing No. 1   Stage 2 End

Bearing length	2.375	inch
Bearing diameter	3.500	inch
Bearing machined radial clearance	.2500D−02	inch
Bearing preload	.0	
Inlet oil temperature	120.0	deg. F
Specified bearing load	320.0	lb
Calculated bearing load	320.1	lb
Bearing eccentricity ratio	.9068D−01	
Minimum film thickness	2.273	mils
Fluid film power loss	1.562	hp
Flow required for 30 degree temperature rise	.6246	gpm
Recommended flow	1.127	gpm
Bearing inlet flow	2.851	gpm
Bearing side flow	1.127	gpm
Bearing net flow	1.127	gpm

Bearing Stiffness Coefficients (lb/inch)			
KXX	KYY	KXY	KYX
1.3964D+06	1.2457D+06	1.0457D+06	−8.9363D+05

Bearing Damping Coefficients (lb-sec/inch)			
BXX	BYY	BXY	BYX
6.0445D+03	5.5037D+03	7.19560+01	7.0321D+01

Sommerfeld number	1.946
Attitude angle (deg.)	36.42
Eccentricity ratio*cos (attitude angle)	.7296D−01
Operating Viscosity, (microreyn)	2.0182D+00
Mean oil temperature, (deg. F)	128.2
Operating oil temperature, (deg. F)	136.3
Fluid film power loss (hp)	1.5616D+00

Table 3. Bearing 2 Steady—State and Dynamic Data

Rotor Speed = 3600.00 rpm
Bearing No. 2   Stage 1 End

Bearing length	2.375	inch
Bearing diameter	3.500	inch
Bearing machined radial clearance	.25000−02	inch
Bearing preload	.0	
Inlet oil temperature	120.0	deg. F
Specified bearing load	220.0	lb
Calculated bearing load	220.0	lb
Bearing eccentricity ratio	.6319D−01	
Minimum film thickness	2.342	mils
Fluid film power loss	1.558	hp
Flow required for 30 degree temperature rise	.6232	gpm
Recommended flow	1.127	gpm
Bearing inlet flow	2.852	gpm
Bearing side flow	1.127	gpm
Bearing net flow	1.127	gpm

Bearing Stiffness Coefficients (lb/inch)			
KXX	KYY	KXY	KYX
1.2092D+06	1.1121D+06	9.0500D+05	−8.0710D+05

Bearing Damping Coefficients (lb-sec/inch)			
BXX	BYY	BXY	BYX
5.2666D+03	4.9210D+03	3.5016D+01	3.3395D+01

Sommerfeld number	2.834
Attitude angle (deg.)	35.82
Eccentricity ratio*cos (attitude angle)	.5124D−01
Operating Viscosity, (microreyn)	2.0195D+00
Mean oil temperature, (deg. F)	128.1
Operating oil temperature, (deg. F)	136.3
Fluid film power loss (hp)	1.5581D+00

carries 220 lbs. The coefficients were calculated using a computer program [1] which iteratively solves the two-dimensional, incompressible Reynolds equation and dynamically perturbs the pressures.

Seal Dynamic Coefficients

The impeller seal rings, or wear rings, experience axial pressure gradients which generate axial turbulent flow in the hydrocarbon working fluid. The flow creates radial and cross-coupling stiffness and damping. This effect is very important in pump dynamics when the pump rotor is relatively long and flexible. The stiffness of the seals provides added support to the rotor and significantly raises the critical speed. In addition to stiffness and damping, a small attached mass effect may exist in the rings. The concentric theory formulated by H. Black [2, 3, 4, 5, 6] in the early 1970s was used for predicting the dynamic properties of seal rings.

The discharge-side seal rings usually exhibit a small axial pressure gradient, and are therefore treated as concentric hydrodynamic journal bearings with fully flooded clearances.

The balance piston was also treated by Black's theory with a correction for the greater axial length. The theory predicts a large added mass effect because the flow remains in the seal for a relatively longer time.

load change. Thus, the major pressure drop occurred over the disk face and little pressure drop remained across the two adjacent wear-ring seals on the hubs of the balance piston and stage 2 impeller. Lacking an appreciable pressure drop, those wear ring seals would not develop radial stiffness or damping and were omitted from the model.

MOD 3—Steel shaft with new balance piston (Figure 3) and five active seals. This model differed from MOD 1 in that the balance disk was replaced by a balance piston. Unlike the balance disk, the balance piston acted like a large bearing, and developed significant radial and cross-coupling stiffness and damping. Also, the pressure drop across the balance piston was unaffected by axial movement of the rotor. Thus, the seal coefficients would remain constant during changes in pump load.

MOD 4—Bronze shaft with five active seals. This model was the same as MOD I except that the shaft was less stiff due to the lower elastic modulus of bronze compared to steel.

The data which define the MOD I model are listed in Table 1. The geometry, stiffness and mass data of the rotor, combined with bearing and seal coefficients, form the input for all critical speed and synchronous response calculations. The three other cases were modelled in similar fashion.

Journal Bearing Coefficients

The journal bearing is depicted in Figure 4. It is a composite, hydrodynamic bearing consisting of tapered-lands cut into a cylindrical bore. The bearing was approximated as a tapered-land bearing. The length was assumed to be the overall length of both the cylindrical and tapered-land sections. The hydronamic effects of the cylindrical sections (which act as axial seals) on the ends of the bearings were assumed to be minimal since the pressure there will be relatively low due to the close proximity to ambient pressure.
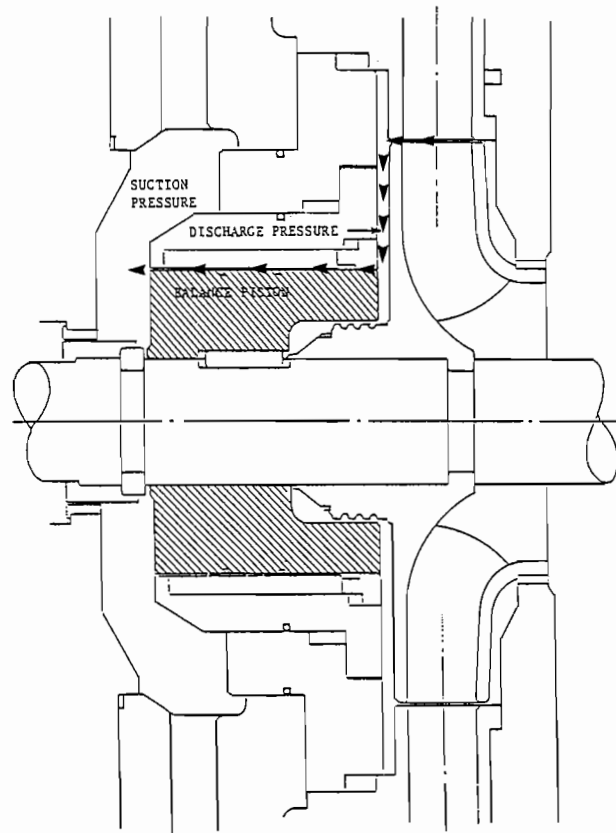

Figure 3. New Design—Balance Piston.

Table 1. Rotor Model—MOD 1.

Mat no. 1	Youngs Mod. (lb/in**2)	Density (lb/in**3)	Shear Mod. (lb/in**2)
1	3.00000+07	2.8300−01	1.04000+07

	Rotor Data									
Stat no.	Mass (lbs)	IP (lb-in**2)	IT (lb-in**2)	Length (in)	Stiff. dia.	Mass dia.	Inner dia.	Youngs Mod. (lb/in**2)	Density (lb/in**3)	Shear Mod. (lb/in**2)zzzz
1	0.0	0.0	0.0	13.500	2.750	2.750	0.0	3.0000D+07	2.830D−01	1.040D+07
2	0.0	0.0	0.0	8.900	3.500	3.500	0.0	3.0000D+07	2.830D−01	1.040D+07
3	7.200D+00	2.8000D+01	5.0000D+01	6.500	3.600	3.600	0.0	3.0000D+07	2.830D−01	1.040D+07
4	0.0	0.0	0.0	0.750	3.000	3.000	0.0	3.0000D+07	2.830D−01	1.040D+07
5	0.0	0.0	0.0	1.600	3.750	3.750	0.0	3.0000D+07	2.830D−01	1.040D+07
6	8.900D+01	1.6860D+03	9.6900D+02	2.150	3.750	3.750	0.0	3.0000D+07	2.830D−01	1.040D+07
7	0.0	0.0	0.0	3.750	3.750	3.750	0.0	3.0000D+07	2.830D−01	1.040D+07
8	0.0	0.0	0.0	2.600	3.750	3.750	0.0	3.0000D+07	2.830D−01	1.040D+07
9	1.000D+02	3.1130D+03	1.9100D+03	0.750	3.250	3.250	0.0	3.0000D+07	2.830D−01	1.040D+07
10	0.0	0.0	0.0	2.250	3.750	3.750	0.0	3.0000D+07	2.830D−01	1.040D+07
11	0.0	0.0	0.0	3.500	3.750	3.750	0.0	3.0000D+07	2.830D−01	1.040D+07
12	0.0	0.0	0.0	2.600	3.750	3.750	0.0	3.0000D+07	2.830D−01	1.040D+07
13	1.000D+02	3.1130D+03	1.9100D+03	3.000	3.750	3.750	0.0	3.0000D+07	2.830D−01	1.040D+07
14	0.0	0.0	0.0	14.400	3.750	3.750	0.0	3.0000D+07	2.830D−01	1.040D+07
15	7.200D+00	2.8000D+01	5.0000D+01	8.900	3.620	3.620	0.0	3.0000D+07	2.830D−01	1.040D+07
16	0.0	0.0	0.0	8.000	3.500	3.500	0.0	3.0000D+07	2.830D−01	1.040D+07
17	0.0	0.0	0.0	2.000	3.500	3.500	0.0	3.0000D+07	2.830D−01	1.040D+07
18	0.0	0.0	0.0	0.010	3.500	3.500	0.0	3.0000D+07	2.830D−01	1.040D+07

Bearing stations
2 7 8 11 12 14 16

Rotor Wt. (lbs)	Rotor IP (lb-in**2)	Rotor IT w/respect to CG (lb-in*h*2)	Brg.1-CG (in)	Distance Brg.1-Brg.2	Rotor Length (in)
5.3754D+02	8.342070D+03	1.536771D+05	29.048	61.6500	85.1500

The calculated stiffness and damping coefficients are summarized in Table 4 for the hub and suction wear ring seals and the balance piston. It should be noted that the balance piston is the dominant contributor to seal stiffness and damping in the MOD 3 configuration.

The API Standard 610 balance specification (2.8.2.4) for this rotor yields 2.3 oz-in of maximum imbalance per plane. This imbalance was used to excite the first natural mode of vibration for this rotor. Semi-amplitude (zero-peak) response to this imbalance placed near the balance piston for MOD 1-4 is depicted in Figures 6, 7, 8, and 9, respectively.

Table 4. Seal Dynamic Coefficients.

	KXX	KXY	KYX	KYY	WBXX	WBXY	WBYX	WBYY
Original balance disk hub seal (lbs/in)	12975	10853	−10853	12975	21705	5677	−5677	21705
New balance piston seal (lbs/in)	22458	129493	−129493	22458	258986	129479	−129479	258986
Stage 2 hub seal (lbs/in)	16253	9342	9342	16253	18685	3172	−3172	18685
Stage 1 hub seal (lbs/in)	11487	7929	−7929	11487	15859	3281	−3281	15859
Stage 1 & 2 suction seal (lbs/in)	24186	10509	−10509	24186	21018	3175	−3175	21018

Analysis Results

The undamped critical speed map for MOD 1 is shown in Figure 5. Seal stiffnesses are included. It is typical of all four models, the only difference among them being a slight variation in the first critical at high stiffness levels. The critical speed map shows that operating speed is close to the first undamped critical speed.

All four response plots show an increase in the critical speed over the undamped critical speeds. The increase is primarily due to seal damping. Bearing damping is relatively ineffective since the relative shaft amplitudes at the bearings are nearly zero. The mode shape at 3,600 rpm for MOD 1 is shown in Figure 10. Note that the shaft nodes occur at the bearings.

The pertinent unbalance response results for the four cases studied are summarized in Table 5.
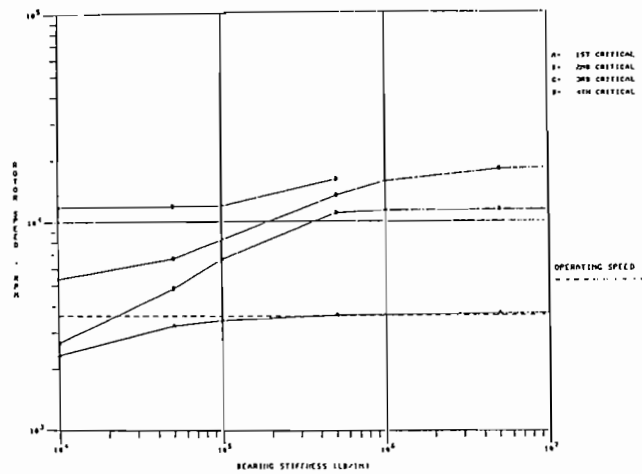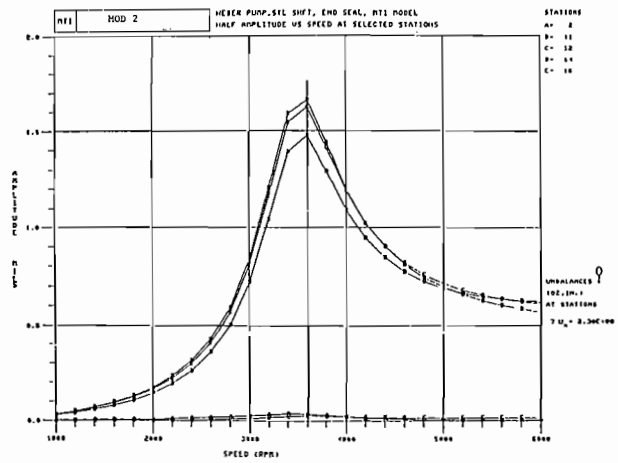

Figure 5. MOD 1 — Critical Speed Map.

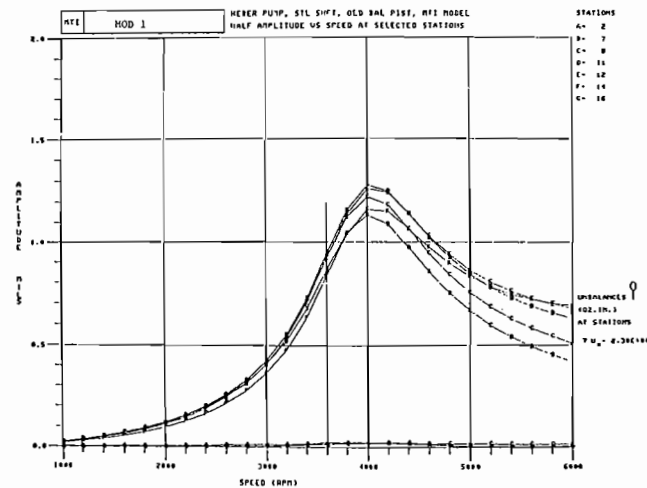*Figure 7. Synchronous Response, MOD 2.*

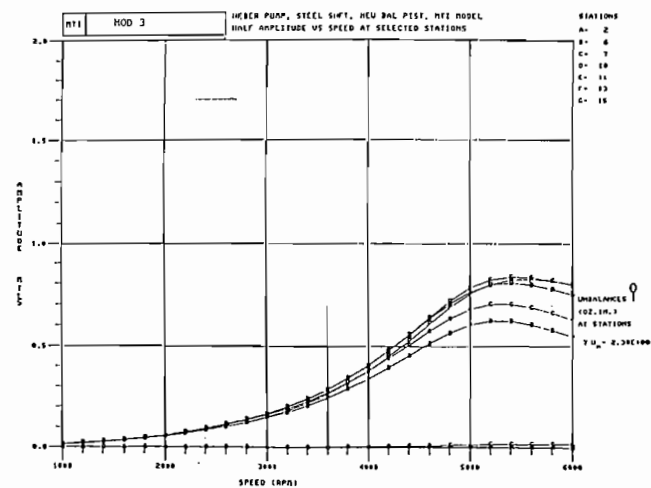*Figure 6. Synchronous Response, MOD 1.*

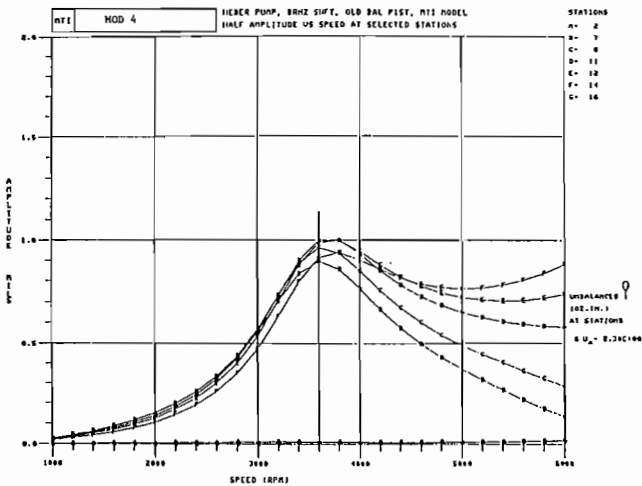*Figure 8. Synchronous Response, MOD 3.*
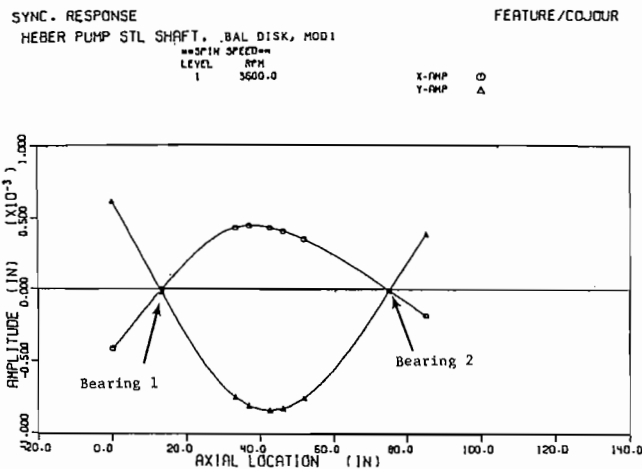
Figure 9. Synchronous Response, MOD 4.

Figure 10. Mode Shape at 3600 RPM, MOD 1.

Table 5. Summary of First Mode Unbalance Response to 2.3 Oz-In at Balance Disk

	Mod. 1	Mod. 2	Mod. 3	Mod. 4
Maximum peak-to-peak response within operating range (mils)	1.8	3.5	0.6	2.0
Speed at maximum response within operating range (rpm)	3,600	3,550	3,600	3,600
Separation margin*	+11%	−1%	+44%	0%
Amplification Factor*	2.90	5.0	N/A**	3.0
Meets A.P.I. 610	no	no	yes	no

**Not applicable
*See Appendix A

DISCUSSION OF ROTORDYNAMICS

The calculations agreed with field measurements of pump behavior. The wet pump rotor with all seals active runs very close to the first critical speed, just below it with a steel shaft, and just above it with a bronze shaft. Furthermore, the rotor mode shape at the first critical speed is that of a flexible rotor on rigid bearings. There is virtually no motion at the bearings, and, therefore, no effective damping. The rotor critical speed and response to unbalance are controlled almost entirely by the stiffness and

damping available from the wear-ring seals. If wear-ring seal clearances increase in service as a result of seal rubs, the stiffness and damping of the seals will decrease and the vibration behavior of the rotor will be degraded.

The unbalance response runs provided the most important insight into the vibration behavior of the pumps. The unbalance response of the original pump rotor (steel shaft and balance disk, Figure 6), shows that at 3600 rpm, the rotor is operating on the steepest part of the response curve just below the critical speed of 4000 rpm. The relatively distinct peak indicates a lightly damped system. A rotor operating with these characteristics would be expected to be sensitive with a tendency toward high vibration, unless balance was exceptionally good.

When the unbalance disk was replaced with a cylindrical balance piston, the response curve became that of Figure 8. The large diameter and close clearance of the piston made it act like a very large bearing with significant stiffness and damping. The effect was to raise the critical speed above 5000 rpm, and to greatly reduce amplitude and slope of the response curve at 3600 rpm. The level of vibration is down by a factor of 3. This explains the reduced steady-state vibration encountered during the brief one-hour test of a balance piston equipped rotor. This is clearly a superior dynamic system.

Replacing the steel shaft with one made of bronze produced the response shown in Figure 9. Here the rotor is operating right on the first critical speed. Again, the slope of the response curve at speeds approaching the critical indicates that this rotor, too, should have a tendency toward high vibration. The amplitude of vibration for the applied level of unbalance is the same as that of the steel shaft in Figure 6.

CAUSE OF LOAD-RELATED VIBRATION

The rotordynamic analysis showed that these pumps have high vibration sensitivity, because they operate very close to the first critical speed and are dependent on the modest damping available in the wear ring seals to control rotor response. However, an additional feature of observed performance remained to be explained. The pumps equipped with balance disks were always sensitive to sudden load increases. Under these conditions they experienced rapid increases in vibration often to the alarm or trip level. The high vibration usually could be reduced by the operator reducing the load on the pump. The balance piston-equipped rotor experienced a sudden large load increase during its one hour run with no increase in vibration.

During the calculation of wear ring seal stiffnesses the reason for this behavior was found. An enlarged view of the balance disk, the seals on the hubs of the disk, and the second stage impeller are shown in Figure 2. It can be seen that the two hub seals and the axial clearance on the disk face form three flow resistances in series. The pressure drop takes place between the second stage discharge pressure and the pump suction pressure at the outboard face of the balance piston. The radial stiffness of the hub seals is proportional to the pressure drop across them. The portion of the total pressure drop attributed to the balance disk is a function of the clearance across the disk face. When a large load increase occurs in the pump, the increased load on the thrust bearing causes the rotor to move toward the suction, decreasing the clearance in the balance disk. The pressure drop across the disk increases which leaves less of the total drop to be taken across the hub seals. Their stiffness declines as a result, and the rotor has less radial support.

This was the mechanism through which pump load and rotor support were coupled. Computer model MOD 2 was created to investigate this effect on rotor vibration. In this limiting case, the stiffness of the hub seals was reduced to zero. The result, shown in Figure 7, was that the critical speed moved downward

to coincide with running speed. The response peaks at a value nearly double the value (shown in Figure 6) due to the decreased damping.

The cause of the increase in vibration with load increase for the balance disk design is now clear. This also explains why no increase in vibration occurred with the balance piston-equipped rotor. There is no change in seal stiffness with axial movement of the balance piston because the piston clearance and pressure drop remain unchanged.

Further reflection on the importance of seal stiffness in controlling rotor critical speed leads to the probable explanation for the gradual increase in vibration of these pumps over time. Each load excursion which leads to a vibration increase probably causes minor seal wipes. Each wipe results in an increase in seal clearance with corresponding drop in seal stiffness and damping. The loss of rotor support lowers the critical speed slightly, which means the rotor is operating closer to the critical and higher on the response curve. This leads to progressive deterioration in rotor performance until it has to be removed from service. It is not surprising then that virtually all rotors removed from service for high vibration had wiped wear ring seals.

CONCLUSIONS

The pump rotors equipped with a balance disk operated very close to their respective first critical speeds. These rotors were sensitive to vibration because the pump rotor is flexible at the first critical speed making bearing damping ineffective.

An increase in pump load (flow) resulted in loss of stiffness and damping in two of the five active seals in those pumps fitted with a balance disk. This was the cause of the increase in rotor vibration with increasing pump load.

The pump fitted with a balance piston was much less sensitive to vibration and was unaffected by load changes. The change from balance disk to balance piston has solved the $1 \times$ vibration problem in these pumps.

APPENDIX A

EXCERPTS FROM SECTION 2.8 OF A.P.I. STANDARD 610 [7]

2.8.1.3 Actual critical speeds shall not encroach upon specified operating speed ranges. The amplification factor (Figure 11) shall not exceed 8 while going through criticals. Values of amplification factors less than 5 are preferred. When specified by the purchaser, this measurement shall be recorded on deceleration (coast down) with the slow-roll (300-600 revolutions per minute) total run-out (electrical and mechanical) subtracted by vectorial run-out compensation. These recorded shaft-relative data shall include speed, peak-to-peak displacement, and phase.

2.8.1.4 The separation margin (Figure 11) of encroachment from all lateral modes (including rigid and bending) shall be at least (1) 20 percent over the maximum continuous speed for rigid rotor systems, or (2) 15 percent below any operating speed and 20 percent above the maximum continuous speed for flexible-shaft rotor systems.
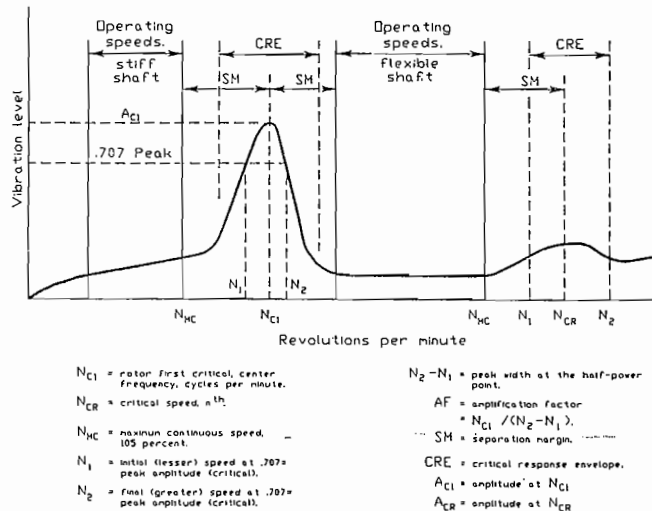

N_{CI} = rotor first critical, center frequency, cycles per minute.
N_{CR} = critical speed, n^{th}.
N_{HC} = maximum continuous speed, 105 percent.
N_1 = initial (lesser) speed at .707 peak amplitude (critical).
N_2 = final (greater) speed at .707 peak amplitude (critical).

$N_2 - N_1$ = peak width at the half-power point.
AF = amplification factor = $N_{CI} / (N_2 - N_1)$.
SM = separation margin.
CRE = critical response envelope.
A_{CI} = amplitude at N_{CI}.
A_{CR} = amplitude at N_{CR}.

Figure 11. Vibration Definitions — From API 610.

REFERENCES

1. Lund, J. W., Koch, E. S., Malanoski, S. B., "Performance of Sector-Lobed Journal Bearings," MTI Computer Program CADENSE 30TL (June 1981).

2. Black, H. F., "Calculation of Forced Whirling and Stability of Centrifugal Pump Rotor Systems," ASME Paper No. 73-DET-131 (1973).

3. Black, H. F., and Jenssen, D. N., "Effects of High Pressure Ring Seals on Pump Rotor Vibrations," ASME Paper No. 71-WA/FE 38 (1971).

4. Black, H. F., "Effects of Hydraulic Forces in Annular Pressure Seals on the Vibrations of Centrifugal Pump Rotors," Journal of Mech. Eng. Science, *II*, (2) (1969).

5. Black, H. J., and Jenssen, D. N., "Dynamic Hybrid Bearing Properties of Annular Pressure Seals," Proc. I, Mech. E., *184* (3N) (1970).

6. Black, H. F., and Cochrance, E. A., "Leakage and Hybrid Bearing Properties of Serrated Seals in Centrifugal Pumps," 6th International Conference on Fluid Sealing, Munich, (1973).

7. API Standard 610, "Centrifugal Pumps for General Refinery Services," Sixth Edition, Washington, D.C.: American Petroleum Institute (1981).

ACKNOWLEDGEMENTS